Available online at www.sciencedirect.com
SCIENCE DIRECT®
Biochimica et Biophysica Acta 1612 (2003) 164–171
BIOCHIMICA ET BIOPHYSICA ACTA
BBA
www.bba-direct.com

# Molecular basis for membrane selectivity of NK-2, a potent peptide antibiotic derived from NK-lysin

Hannah Schröder-Borm[a], Regine Willumeit[b], Klaus Brandenburg[c], Jörg Andrä[a,c,*]

[a] *Department of Biochemistry and Molecular Biology, University of Hamburg, Hamburg, Germany*
[b] *GKSS Research Center, Geesthacht, Germany*
[c] *Biophysics Division, Forschungszentrum Borstel, Borstel, Germany*

Received 13 March 2003; accepted 4 April 2003

**Abstract**

Increasing resistance of pathogenic bacteria against antibiotics is a severe problem in health care. Natural antimicrobial peptides and derivatives thereof have emerged as promising candidates for ''new antibiotics''. In contrast to classical antibiotics, these peptides act by direct physical destabilization of the target cell membrane. Nevertheless, they exhibit a high specificity for bacteria over mammalian cells. However, the precise mechanism of action and the molecular basis for membrane selectivity are still a matter of debate. We have designed a new peptide antibiotic (NK-2) with enhanced antimicrobial activity based on an effector protein of mammalian immune cells (NK-lysin). Here we describe the interaction of this α-helical synthetic peptide with membrane mimetic systems, designed to mimic the lipid compositions of mammalian and bacterial cytoplasmic membranes. Utilizing fluorescence and biosensor assays, we could show that on one hand, NK-2 strongly interacts with negatively charged membranes; on the other hand, NK-2 is able to discriminate, without the necessity of negative charges, between the zwitterionic phospholipids phosphatidylethanolamine (PE) and phosphatidylcholine (PC), the major constituents of the outer leaflet of the cytoplasmic membranes of bacteria and mammalian cells, respectively.


*Keywords:* Antibacterial peptide; Peptide antibiotic; Model membrane; NK-lysin; Melittin

## 1. Introduction

Natural antimicrobial peptides are part of the innate immunity of a wide range of species ranging from insects over amphibia to mammalia, including humans. They provide a first line of defense against infections with bacteria, fungi, parasites and enveloped viruses, and some peptides are even effective against tumor cells (for reviews see [1–6]). Though their precise mechanism of action is not fully understood, it is widely accepted that the target membrane is the scene of action, without the exploitation of a specific receptor [7]. This mechanism differentiates them from classical antibiotics and is presumably the main reason for the insignificant development of microbial resistance against these ''new antibiotics'' [8]. Therefore, natural peptide antibiotics and synthetic analogs thereof have emerged as compounds with potentially significant therapeutical applications against human pathogens [9–11].

Antimicrobial peptides are typically small (15–50 amino acid residues) but have a diverse fold, such as α-helices, β-sheets and cyclic structures. However, they share an overall amphipathicity and a positive net charge, which are thought to be prerequisites for the interaction with the negatively charged membranes of bacteria [12,13]. Among the hundreds of natural peptides isolated so far (seehttp://www.bbcm.univ.trieste.it/~tossi/pag1.htm), mammalian defensins [14], magainins of amphibia [15] and the insect cecropins [16] are the most prominent representatives. Different models for the peptide/membrane interaction have been suggested in the literature: For lower peptide/lipid ratios it has been shown that magainins and cecropin A are associated with the lipid headgroups, oriented in parallel to the membrane [17,18], and thus cover the membrane like a carpet (carpet model [19]). However, at a distinct peptide/lipid ratio, some peptides seem to penetrate the bilayer and are then oriented perpendicular to

*Abbreviations:* FTIR, Fourier-transformed infrared spectroscopy; LUV, large unilamellar vesicle; PC, L-α-phosphatidylcholine; PE, L-α-phosphatidylethanolamine; PG, L-α-phosphatidyl-DL-glycerol; Trp, L-tryptophan

* Corresponding author. Biophysics Division, Forschungszentrum Borstel, Center for Medicine and Biosciences, Parkallee 10, D-23845 Borstel, Germany. Tel.: +49-4537-188280; fax: +49-4537-188632.
*E-mail address:* joerg.andrae@fz-borstel.de (J. Andrä).

0005-2736/03/$ - see front matter © 2003 Elsevier Science B.V. All rights reserved.
doi:10.1016/S0005-2736(03)00115-9

the membrane [20]. In the case of magainin 2, the insertion of peptide results in the formation of a toroidal-like pore, where the peptide is still located at the lipid headgroups, which are now lining, together with the peptides, the inside of the pore (toroidal or wormhole model [21,22]). Besides these very similar carpet-like models, also the formation of distinct pores has been observed in the case of some peptides (barrel-stave model [23]). Even intracellular targets have been identified, if the peptides are able to surmount the cytoplasmic membrane [7,24].

We have constructed a synthetic short version of NK-lysin, a cytolytic and antimicrobial polypeptide of porcine cytotoxic lymphocytes [25], which represents the cationic core region of this potent effector molecule [26]. NK-lysin belongs to the saposin-like proteins (SAPLIPs), a family of 8–9 kDa proteins, structurally conserved, but functionally diverse [27], i.e they share a common α-helical fold with a conserved half-cysteine pattern [28–30]. Besides the name-giving saposins and other related proteins, a particular group of cytotoxic and antibacterial effector molecules of professional killer cells belongs to that family: Amoebapores, isolated from the pathogenic amoeba *Entamoeba histolytica* [31], Granulysin from human T-cells [32], and the aforementioned NK-lysin [25]. These proteins are stored in respective cellular cytotoxic granules and secreted upon contact with a victim cell. In a previous study, we identified the helical core region of the Amoebapore isoform A (H3, residues 40–65) as mediator of its antibacterial and cytotoxic activities [33]. Using a set of synthetic peptides, we further improved the activity and also the selectivity of peptide H3 [34]. Furthermore, we were prompted, by the striking homology of Amoebapores with NK-lysin [35], to construct an H3-like peptide also on the basis of the NK-lysin sequence. Interestingly, this synthetic 27-residue peptide and shortened analog of NK-lysin, termed NK-2, displayed potent activity against clinical isolates of *Candida albicans*, bacteria [26], and also against the protozoan parasite *Trypanosoma cruzi* [36], but was of low toxicity to human cells [26, 36]. We showed by circular dichroism that NK-2 has a random coiled conformation in solution, but adopts an amphipathic α-helical structure in hydrophobic environment [26]. The NK-2 corresponding region of the NK-lysin 3D-structure, extracted from the protein data bank (1NKL), revealed a helix–hinge–helix fold of the peptide (Fig. 1), resembling the structure of cecropin A [37].

Here, we investigated the molecular basis for the selectivity of the synthetic peptide NK-2 utilizing model systems mimicking the eukaryotic and prokaryotic cytoplasmic membranes. The phospholipid compositions of these membranes differ markedly. The architecture of the human erythrocyte cytoplasmic membrane is asymmetric with the inner leaflet predominantly consisting of the amino phospholipids phosphatidylethanolamine (PE) and small amounts of negatively charged phosphatidylserine, and the outer leaflet lacking negatively charged phospholipids but consisting of the choline phospholipids phosphatidylcholine (PC)

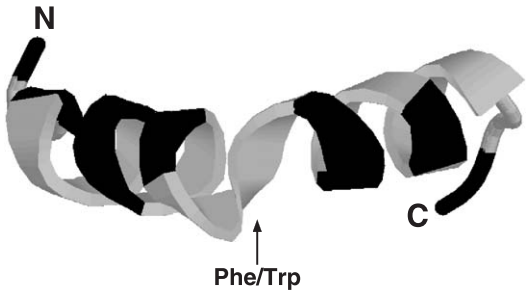


Fig. 1. Structure model of the peptide NK-2. The darkened positively charged lysine and arginine residues illustrate the segregation of hydrophilic and hydrophobic residues. The position of the phe/trp exchange in peptide trpNK-2 is indicated. The structure shown was extracted from the NMR structure of NK-lysin (residues 39–65) deposited at the PDB (1NKL). Please note that the sequence of the peptide NK-2 differs from NK-lysin in three positions (see also Table 1). The α-helical content of the peptide NK-2 was verified by CD spectroscopy [26] and FTIR spectroscopy (this study).

and sphingomyelin ([38] and references therein). In contrast, the cytoplasmic membrane of bacteria is essentially a mixture of PE and negatively charged phosphatidylglycerol (PG) and cardiolipin (between 20% and 100% of total plasma membrane phospholipids [38]). The situation is even more complex due to the existence of the Gram-negative outer membrane, whose outer leaflet is formed nearly exclusively of lipopolysaccharides. Here, as a first approximation to the biological system, we used the zwitterionic phospholipid PC to mimic the human erythrocyte membrane, and a mixture of zwitterionic PE and negatively charged PG for the plasma membrane mimetic of Gram-negative bacteria.

The results we present will show clearly that the peptide NK-2 specifically interacts with the constituents of the bacterial cytoplasmic membrane but not with the ones of the human erythrocyte membrane; negative charges promote this interaction but are not necessary. To allow comparison with other investigations, we frequently used bee venom melittin as a control peptide.

## 2. Materials and methods

### 2.1. Materials

Phospholipids (2-oleoyl-1-palmitoyl-*sn*-glycero-3-phosphocholine, POPC; 2-oleoyl-1-palmitoyl-*sn*-glycero-3-phosphoethanolamine, POPE; 2-oleoyl-1-palmitoyl-*sn*-glycero-3-phospho-rac-(1-glycerol), POPG), and agarose (low electroendosmosis type) were purchased from Sigma (Deisenhofen, Germany). Trypticase soy broth was from Gibco (Karlsruhe, Germany). All other chemicals were of analytical grade from Merck (Darmstadt, Germany).

### 2.2. Peptides and peptide analysis

Melittin (*Apis mellifera*) was purchased as synthetic peptide from Sigma in HPLC-grade and used without

further purification. NK-2 and trpNK-2 were obtained from WITA GmbH (Berlin, Germany) in a purity grade >95%. Their homogeneity was confirmed by analytical RP-HPLC (Lichrospher 100 RP 18, 5-μm column, Merck), MALDI-TOF (Bruker Daltonik GmbH, both performed by the manufacturer), and N-terminal Edman degradation (Procise Protein Sequencing System, Applied Biosystems, Germany). The peptides were synthesized with an amidated C terminus. Mean hydrophobicity and mean hydrophobic moments of the entire peptides were calculated using the Eisenberg consensus scale for hydrophobicity [39]. The existence of a free, non-disulfide bridged, sole cysteine residue in the peptides, under the experimental conditions, was confirmed by reactivity to the Ellman reagent [40] and by MALDI-TOF (BIFLEX, Bruker, Karlsruhe, Germany, performed by N. Nagorny, Institute of Organic Chemistry, University of Hamburg).

### 2.3. Fourier-transformed infrared spectroscopy (FTIR)

The FTIR measurements were performed on an Equinox-55 spectrometer (Bruker) in connection with an AquaSpec flow cell (micro-biolytics GmbH, Freiburg, Germany) at 27 °C. Peptides were applied to repeated cycles of solubilization in 10 mM HCl, liquid nitrogen, and lyophilization to remove any trapped TFA, which would interfere with the FTIR measurements, and finally dissolved in $H_2O$ or $D_2O$ (5 mM). Interferograms (50) were accumulated, apodized, Fourier-transformed and converted to absorbance spectra. The secondary structure was determined by analyzing the amide I-vibration (predominantly C=O stretching vibration). For this two different methods were applied: (i) Curve fitting was done in the spectral range 1700–1600 $cm^{-1}$ using a modified version of the CURFIT program obtained by D. Moffat, NRC, Ottawa, Canada. The bandshapes of the single components are superpositions of Gaussian and Lorentzian. Best fits were obtained by assuming a Gauss fraction of 0.55–0.60. The precision of the curve fit procedure is approximately 3%; and (ii) a calibration was performed in the spectral region 1800–1275 $cm^{-1}$ using the alpha_helix.q2 method and the corresponding protein spectra library of the OPUS/QUANT software package (Bruker).

### 2.4. Assay for antibacterial activity

Antibacterial activity was determined by a radial diffusion assay [41]. The two different layers of the assay both contained 1% agarose, buffered with 10 mM sodium phosphate, pH 7.4, and were autoclaved before seeding of the bacteria. The underlayer agar was supplemented with 0.03% trypticase soy broth, 0.02% Tween 20, and contained $10^5$ cfu/ml of log-phase *E. coli* (ATCC 23716). The overlayer agar was supplemented with 6% trypticase soy broth. Underlayer agar (10 ml) was filled in a squared petri dish (12 × 12 cm); holes with 3.5-mm diameter were punched into the solidified agarose which were filled with 5 μl of the sample. After an incubation period of 3 h at 37 °C, the plate was covered with 10-ml overlayer agar. The plates were incubated overnight at 37 °C. Inhibition zones were expressed in units, with one unit defined as diameter of clearance in millimeter (minus 3.5 mm of the sample containing hole) multiplied by 10.

### 2.5. Assay for hemolytic activity

Freshly collected human erythrocytes were washed with phosphate-buffered saline (10 mM sodium phosphate, 2 mM potassium chloride, 138 mM sodium chloride, pH 7.4), and resuspended in MES-buffered saline (20 mM MES, 140 mM sodium chloride, pH 5.5, $5 \times 10^8$/ml). Subsequently, 20 μl of this erythrocyte suspension was incubated with 80 μl of peptide solution in the same buffer for 30 min at 37 °C. For controls, erythrocytes were incubated with distilled water (maximal lysis) and buffer alone (spontaneous lysis). Lysis was determined by measuring the concentration of released hemoglobin at 412 nm. Percent lysis was defined as (experimental lysis − spontaneous lysis)/(maximal lysis − spontaneous lysis) × 100.

### 2.6. Preparation of lipid vesicles (LUV)

Pure phospholipids or mixtures thereof (2.5 mg) were dissolved in chloroform/methanol (2:1, by volume), the solvent was removed by a constant stream of nitrogen, and the resulting lipid film was dried under vacuum overnight. Subsequently, the lipid film was hydrated in buffer (10 mM sodium phosphate, pH 7.4) to reach a final concentration of 2 mM phospholipid. The suspension was subjected to four freeze-and-thaw cycles with liquid nitrogen and a waterbath of 37 °C, and passed through a 100-nm membrane for 17 times using a liposome extruder (LiposoFast, Avestin Inc., Ottawa, Canada).

### 2.7. Liposome lysis assay

LUVs were prepared as described above, with the variation of the lipid films being hydrated in buffer (10 mM HEPES, 1 mM EDTA, pH 7.4) containing 30 mM calcein (Molecular Probes, Leiden, Netherlands). After extrusion, the liposomes were passed over a PD-10 column (Amersham Bioscience, Freiburg, Germany) to remove untrapped calcein. Elution was done with 10 mM HEPES, 150 mM NaCl, 1 mM EDTA, pH 7.4. Lipid concentration was determined using a phosphorus assay [42]. Liposomes (2.5 μM of phospholipids) were treated with various amounts of peptide at 20 °C and the peptide-induced lysis was monitored fluorometrically by the detection of fluorescent dye release at excitation and emission wavelengths of 490 and 520 nm, respectively (Aminco SPF-500). After signals have been recorded for 10 min ($F_{exp}$), complete dye release was achieved by treatment of liposomes with 0.1% Triton X-

100 ($F_{100\%}$). Spontaneous dye release from liposomes during the time of the experiment (20 min) was less than 2%. Percent lysis was calculated as $(F_{exp} - F_0)/(F_{100\%} - F_0) \times 100$. $F_0$ was the fluorescence level before the addition of peptide.

### 2.8. Biosensor measurements

The optical biosensor IAsys (Thermo Labsystems, Cambridge, UK) uses the resonant mirror technique to monitor the direct molecular interaction of a ligand with a surface in real time. Binding and dissociation events are seen as increasing and decreasing shifts in resonance angle given in arc seconds (arc sec). In our approach, we used a two-well cuvette system with hydrophobic coated surfaces. Lipid monolayers were deposited on the surface from chloroform solutions (lipid concentration 20 mg/ml) using the manufacturer's protocol. The deposition was followed by washes of 50% sucrose (w/v), buffer (10 mM sodium phosphate, 1 mM EDTA, pH 7.4), 100 mM HCl, buffer, 10 mM NaOH, and again buffer. Lipid deposition and all measurements were done at 28 °C. After the baseline was stable, the amount of lipid on the surface was determined and typically was around 1000 arc sec. The homogeneity of the surface was routinely checked by resonance scans. Only surfaces which give a single peak were used for the measurements. Peptide was added to give a final concentration of 1 μM and the increasing signal was monitored over time. Repeated binding experiments were done on freshly prepared monolayers.

### 2.9. Intrinsic tryptophan fluorescence measurements

Intrinsic tryptophan fluorescence was measured using an Aminco SPF-500 spectrofluorometer. Peptides (5 μM) were dissolved in buffer (10 mM sodium phosphate, pH 7.4). Liposomes (LUV) were added to a final molar ratio as indicated. The samples (500 μl) were equilibrated at 27 °C for 5 min. Excitation was done at 280 nm and emission was recorded from 300 to 500 nm. Both slits were set to 4 nm. The spectra of all peptide/liposome mixtures were corrected by subtracting the emission spectra of a liposome suspension of the respective concentration. Data were fitted to a log-normal distribution (proFit 5.1.2, Quantum Soft, Zürich, Switzerland) and $\lambda_{max}$ was obtained from the fitted curves. As a control for artificial wavelength shifts due to scattering effect of the liposome suspension, we recorded spectra of free Trp (5 μM). Only in the presence of a 300-fold molar excess of phospholipids a minimal artificial blue-shift was observed (0.5 to 1.7 nm).

## 3. Results

### 3.1. Peptide construction and structural analysis

The sequence of the antibacterial and candidacidal peptide NK-2 was derived from the core region (residues 39–65) of NK-lysin. It spans its third and fourth α-helical domain including the (mostly positively charged) adjacent amino acid residues. The solution structure of the peptide was determined in $H_2O$ and $D_2O$ by FTIR spectroscopy (Fig. 2A). Since random coil contribution could superimpose to the helical contribution in $H_2O$, we performed secondary structure analysis in $D_2O$ (Fig. 2B). Dissection of the amide I-vibration band of NK-2 into single component bands revealed a strong band centered around 1648 $cm^{-1}$ and minor bands at 1669, 1637 and 1607 $cm^{-1}$, indicating a high portion of α-helical secondary structure (48.6%). A very similar amount of α-helical content (51.0%) was obtained by applying a quantitative method (OPUS/QUANT) based on the comparison of a protein spectra library of known structures. For the analysis of its membrane interaction by fluorescence spectroscopy, we

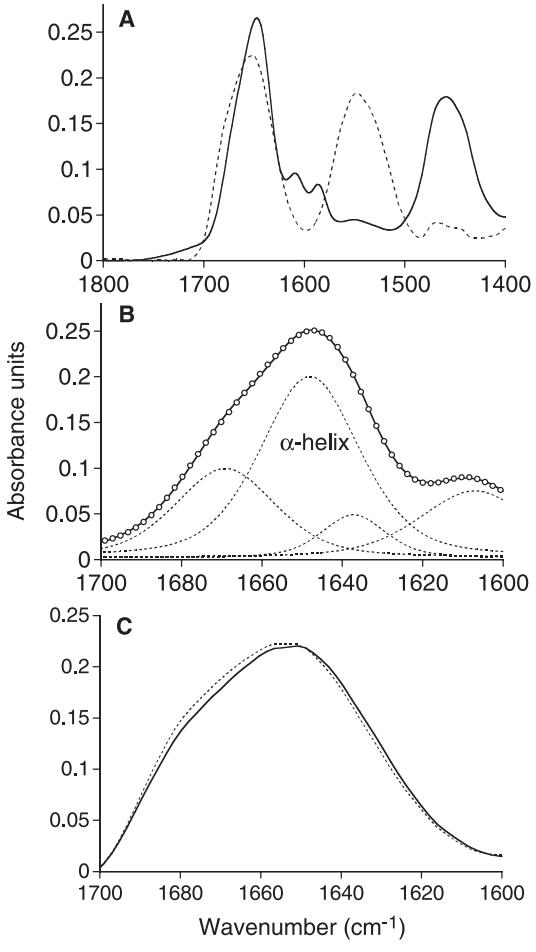


Fig. 2. Secondary structure analysis. Peptide secondary structure was determined by FTIR spectroscopy by analyzing the amide I-vibration. (A) Spectral range of amide I and II (C=O) stretching vibrations of NK-2 (5 mM) in $H_2O$ (dashed line) and $D_2O$ (solid line). (B) Band shape analysis of amide I stretching vibration (open circles) of NK-2 (5 mM) in $D_2O$. The curve fit (solid line) and the single component bands (dashed lines) are shown. The major single component band is centered around 1648 $cm^{-1}$ and can be assigned to an α-helical secondary structure. (C) Amide I stretching vibration of NK-2 (solid line) and trpNK-2 (dashed line) solubilized in $H_2O$ (5 mM).

Table 1
Peptide used in this study

| Peptide | Sequence | | | | | | Residues | Net charge | *H* | <*μ*> |
|---|---|---|---|---|---|---|---|---|---|---|
| NK-2 | KILRG | VCKKI | MRTFL | RRISK | DILTG | KK | 27 | +10 | -0.28 | 0.42 |
| trpNK-2 | ----- | ----- | ---W- | ----- | ----- | -- | 27 | +10 | -0.29 | 0.41 |
| NK-lysin* | ----- | L---- | --S-- | ----W | ----- | -- | | | | |
| Melittin | GIGAV | LKVLT | TGLPA | LISWI | KRKRQ | Q | 26 | +6 | 0.15 | 0.34 |

Residues identical to the NK-2 sequence are indicated by a hyphen. Net charges of the peptides were calculated by counting the amino terminus, arginine and lysine as positive charges, and aspartic acid residues as negative charges (there is no glutamic acid residue in any peptide); *H*, mean hydrophobicity; ⟨*μ*⟩, mean hydrophobic moment; *, partial sequence of NK-lysin (residues 39–65) [25].

introduced an environment-sensitive label into the peptide NK-2; i.e. we substituted a phenylalanine by a tryptophan residue (trpNK-2). This exchange neither influenced the hydrophobic properties of the peptide (Table 1) nor its secondary structure, indicated by an identical shape of the amide I-vibration band determined by FTIR-spectroscopy (Fig. 2C). Though both peptides contain a sole cysteine residue, intermolecular disulfide formation was not observed under the experimental conditions (not shown).

### 3.2. Biological activity

The two synthetic peptides, NK-2 and trpNK-2, were nearly indistinguishable concerning their antibacterial and hemolytic activities (Fig. 3). Both were active against *E. coli* at a similar concentration as melittin, a highly antibacterial and hemolytic peptide from bee venom. However, in contrast to melittin, the NK-2 peptides were not hemolytic to human erythrocytes.

### 3.3. Membrane permeabilization

Release of the fluorescent dye calcein from LUVs of a defined lipid composition after the addition of peptide was monitored over the time. We used liposomes composed of zwitterionic PC and of a mixture of zwitterionic PE and negatively charged PG to mimic the outer layer of human erythrocytes and the bacterial cytoplasmic membrane, respectively. Whereas NK-2 was very effective to evoke calcein release from the negatively charged liposomes (PE/PG), virtually no release was observed with LUVs composed of pure PC (Fig. 4). In contrast, bee venom melittin

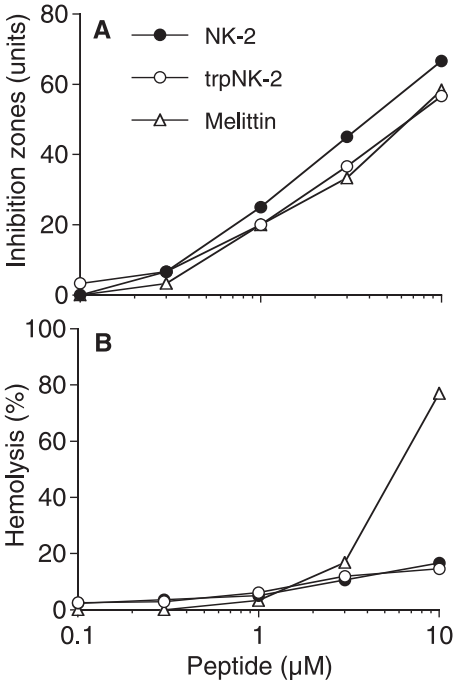


Fig. 3. Antibacterial and hemolytic activities of synthetic peptides. (A) Antibacterial activity was determined in a radial diffusion assay. Here, an inhibition zone of 0.1 mm is defined as one unit. (B) Hemolytic activity was determined by measuring the release of hemoglobin after incubation of the peptides with human erythrocytes for 30 min at 37 °C. Values were determined in duplicates at least in two independent experiments.

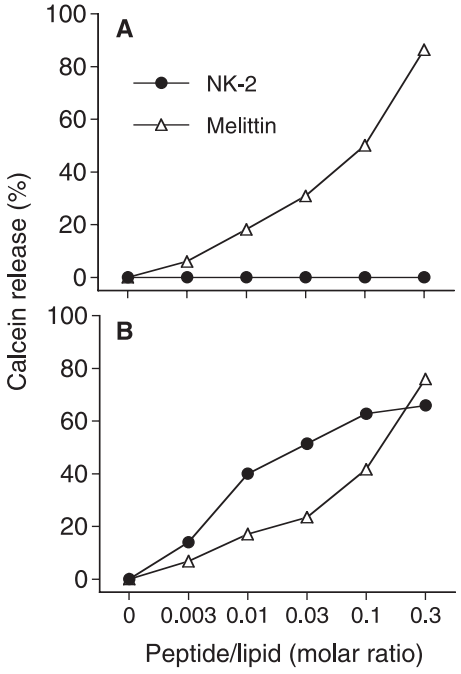


Fig. 4. NK-2 induced liposome lysis. Peptide induced lysis of calcein containing LUVs made of (A) PC and of (B) a molar 80:20 mixture of PE/PG monitored fluorometrically by the detection of dye release at room temperature. Percent leakage was calculated then as described in Material and methods and presented here dependent on the lipid/peptide molar ratio. For comparison, melittin was used at the same concentrations.

did not discriminate between the two types of membranes and evokes liposome leakage irrespective of its lipid composition (Fig. 4).

### 3.4. Membrane binding kinetics

In order to discriminate between membrane association, insertion and lysis, we first analyzed the binding kinetics of the peptide NK-2 on lipid monolayers utilizing a biosensor system. Monolayers were generated on a hydrophobic surface cuvette, NK-2 was added and the amount of bound peptide was monitored in real time by the resonant mirror technique. Monolayers consist of pure PC or PE and a 80:20 molar mixture of PE/PG. An increasing signal, corresponding to the amount of bound peptide, was seen with PE/PG, but also with pure PE monolayers. Virtually no interaction was observed with pure PC (Fig. 5). A critical step in biosensor experiments is the regeneration of the used surface, i.e., in our case the removal of the peptide from the lipid monolayer. We tried to do this by treatment with multiple cycles of high salt, NaOH and HCl. In the case of NK-2 bound to the PE/PG monolayer, this procedure did not result in a decrease of the binding signal, indicating that the peptide could not be removed. However, NK-2 bound to PE was detached from the monolayer by three or four washing cycles with HCl and buffer, as evidenced by a signal drop back to the membrane level (not shown).

### 3.5. Membrane binding mode

Fluorescence emission spectra were recorded, after excitation at 280 nm, for trpNK-2, melittin and L-tryptophan (Trp) as a reference. The wavelengths of the emission maxima ($\lambda_{max}$) of trpNK-2 and melittin in buffer alone were 345.4 and 348.4 nm, respectively ($n=19$), and very similar to $\lambda_{max}$ of free Trp (350.0 nm, $n=3$), thus indicating full solvent exposure of the tryptophan side chains in trpNK-2 and melittin (Fig. 6A). Lipid vesicles were added then in great molar excess (30- to 300-fold) to guarantee full saturation of peptide with lipids. The phospholipid composition of the vesicles had a strong influence on the emission spectra of trpNK-2 (Fig. 6B). At a 30-fold molar excess of phospholipids: (i) a strong blue-shift ($\lambda_{max}=328.1$ nm), indicating a membrane-buried tryptophan, was observed in the presence of negatively charged LUVs (PE/PG); and (ii) a slight shifting ($\lambda_{max}=338.8$ nm), indicating a semi-exposed trp side chain, was observed in the presence of pure zwitterionic PE; whereas (iii) virtually no shift was seen with LUVs of pure zwitterionic PC up to a 300-fold molar excess (Fig. 6B). For comparison, the trp-fluorescence emission of melittin also was strongly affected after addition of LUV, but was more or less independent of the liposome phospholipid composition (not shown).

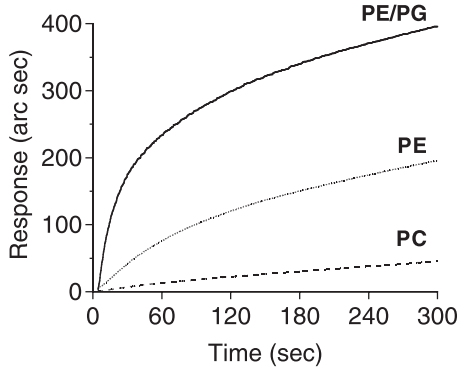


Fig. 5. Membrane binding kinetics of NK-2. The peptide NK-2 was added to a biosensor surface covered with monolayers of PC, PE or a molar 80:20 mixture of PE/PG. The increasing binding signal (Response, arc sec) was recorded over time.

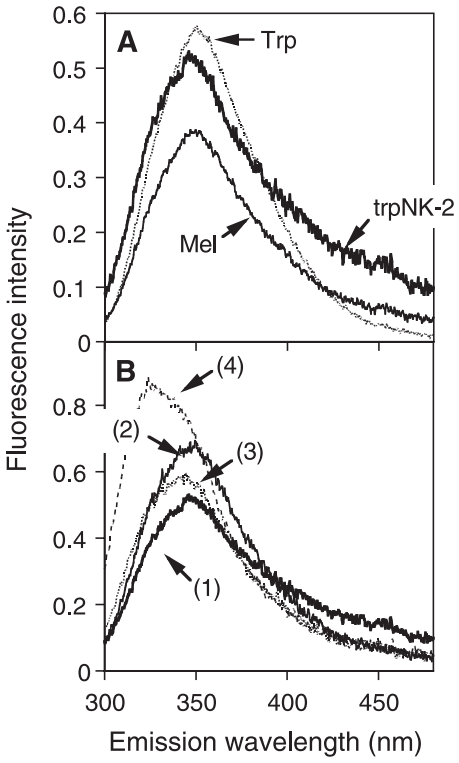


Fig. 6. Intrinsic tryptophan fluorescence. After excitation at 280 nm, fluorescence emission spectra were recorded in the absence of lipids (A) for trpNK-2, melittin (Mel), and L-tryptophan (Trp). (B) Emission spectra of trpNK-2 in the absence (1) and presence of LUVs, at a 30-fold molar excess of phospholipids consisting of PC (2), PE (3) and a molar 80:20 mixture of PE/PG (4).

## 4. Discussion

We have shown previously that the peptide NK-2 is very effective against several strains of bacteria and *Candida* with inhibitory concentrations of less than 1 μM, but is virtually inactive against human erythrocytes and keratinocytes [26]. The main site of action is the target cell membrane as demonstrated by liposome lysis experiments [26]. Therefore, it seems reasonable to suppose that the

peptide's selective membranolytic activity is based on differences in target cell membrane composition. To elucidate this selectivity, we used model biomembranes of a distinct phospholipid composition mimicking mammalian or bacterial cytoplasmic membranes. In this paper, we focussed our investigations on NK-2 interactions with the different phospholipid headgroups, albeit it has been shown that interaction of peptides can also be affected by the alkyl chain composition. To avoid this problem, we used identical alkyl chains (PO = palmitoyl, oleoyl) for all phospholipids throughout this work. Our experimental models include dye release from unilamellar lipid vesicles (LUV), peptide binding to lipid monolayers on a biosensor surface, and the change in fluorescence emission of an intrinsic tryptophan residue after association to LUV.

The results obtained by the three different methods concur in their major statement, and are in a good correlation to the antibacterial, hemolytic, cytotoxic and candidacidal data ascertained for NK-2 so far (Ref. [26] and this study). Obviously, NK-2 is able to discriminate between different cell types based on different compositions of their respective lipid matrix. It seems clear that a strong electrostatic interaction of the cationic peptide and a negatively charged membrane surface promotes the peptide/membrane association. We already have found such a preference for the Amoebapores [43,44] and derivatives thereof [33,34], and this has also been reported for the cecropins [13], defensins [12,45] and various other peptides. However, our biosensor experiments also revealed a binding capability of NK-2 for the zwitterionic PE surface (the amount of bound peptide reaches approximately 1/3 the level of the negatively charged PE/PG surface), whereas virtually no NK-2 binding was observed to the PC monolayer. This PC vs. PE discrimination was surprising, but was verified subsequently by following the changes of the intrinsic tryptophan fluorescence during peptide/liposome interaction, and raises the following question: How does NK-2 distinguish between the identical charged and chemically very similar structured PC and PE headgroups? One important difference between PC and PE is their head group geometry [46]. Whereas both phospholipids form lamellar lipid phases at physiological temperatures, the cone-shaped PE causes a negative membrane curvature and thus promotes the formation of non-lamellar, inverted lipid phases at higher temperatures. It is suggestive to think that NK-2 binding would promote this curvature strain, which subsequently leads to the collapse of the bacterial cytoplasmic membrane. For other lytic peptides, a stabilizing (magainin 2 [47]) as well as a destabilizing (gramicidin S [48]) influence on the lamellar phase of PE has been observed. However, these differences in lipid phase behaviour might explain the differences in NK-2-induced membrane lysis, for instance in the antibacterial vs. hemolytic assay, albeit they do not explain the differences in NK-2 attachment to the model membranes. Possibly, the voluminous trimethylamine umbrella of the choline group shields the negative charge of the phosphate group more efficiently than does the amine group of the ethanolamine moiety. This could result in local negative charges on the PE membrane which facilitates binding of the positively charged peptide.

The fluorescence of the tryptophan side chain is sensitive to the polarity of the environment and thus is a powerful tool to study the microenvironment of amino acid residues in proteins (see Ref. [49] and references therein). Weak and strong wavelength shifts of the Trp emission maximum allow to distinguish between semi exposed and fully membrane buried Trp side chains, respectively [50]. The peptide NK-2 lacks a tryptophan residue; however, we introduced a sole Trp residue as an intrinsic fluorescence probe by substituting the phenylalanine residue in position 14 (see also Fig. 1 and Table 1). From a hydrophobic point of view, this phe/trp substitution is rather conservative, and consequently no dramatic changes in activity were found by our biological assays. Analysis of the secondary structure of NK-2 and the tryptophan variant trpNK-2 by FTIR-spectroscopy revealed a nearly identical amide I vibration band, indicating, first, that no structural changes occur due to the amino acid exchange, and second, that both peptides have an high content of α-helical structure in water (i.e. in a hydrophilic environment). This finding is somewhat differing to CD-spectroscopy data obtained earlier, where we found an α-helical structure for NK-2 only in the presence of trifluoroethanol (hydrophobic environment) [26]. However, the peptide concentration was approximately 15 times lower in the CD experiment compared to the FTIR measurements, which might influence the formation of a defined secondary structure [51]. The fluorescence data obtained suggest a superficial membrane interaction for trpNK-2 with PE liposomes (semi-exposed trp), but a strong hydrophobic environment for the trp side chain (i.e. a membrane-buried trp) if negatively charged phospholipids (PG) are present. A congruent interpretation can be drawn from the biosensor data: on one hand, NK-2 could be removed from the PE monolayer, i.e. a superficial attachment of the peptide; on the other hand, regeneration failed for the PE/PG monolayer, the peptide must stick strongly on, or penetrate into the lipid layer.

We conclude, and it is likely, that similar factors, as found for its shortened analog NK-2, also determine the membrane selectivity of NK-lysin; on the molecular level, the target cell specificity of NK-2 only partly is based on an electrostatic interaction between the positively charged side chains of the peptide and the negatively charged membrane, which have been made responsible for the action of many antibacterial peptides on the bacterial cytoplasmic membrane [9,52]. Anionic charges promote membrane binding of the peptide and are necessary to manifest a strong interaction/penetration of NK-2; this could also hold true for zwitterionic PE as discussed above. On the other hand, the postulated wedge geometry of NK-2 (Fig. 1), in combination with the particular segregation of cationic and hydro-

phobic amino acid residues on the outside and inside of the alpha-helix, respectively, would allow to enhance the intrinsic negative curvature strain of a PE lamellar phase. Other membrane components, particularly the presence of cholesterol exclusively in the eukaryotic membrane, may further improve the peptide target selectivity as it has been reported for magainin 2 [53]. The discrimination between PE and PC, the major ('uncharged') phospholipid constituents of bacterial and human plasma membranes, respectively, is an inherent, interesting feature of NK-2 and needs further investigations.

## Acknowledgements

We thank Nathalie Jänner, Till Kortüm and Kay Oetzmann for experimental help, and Dr. Manfred Teppke for N-terminal sequencing of the peptides.

## References

[1] H.G. Boman, Annu. Rev. Immunol. 13 (1995) 61–92.
[2] D. Andreu, L. Rivas, Biopolymers 47 (1998) 415–433.
[3] R.E.W. Hancock, Lancet 349 (1997) 418–422.
[4] R.E.W. Hancock, D.S. Chapple, Antimicrob. Agents Chemother. 43 (1999) 1317–1323.
[5] W. van't Hof, E.C. Veerman, E.J. Helmerhorst, A.V. Amerongen, Biol. Chem. 382 (2001) 597–619.
[6] M. Zasloff, Nature 415 (2002) 389–395.
[7] R.M. Epand, H.J. Vogel, Biochim. Biophys. Acta 1462 (1999) 11–28.
[8] D.A. Devine, R.E. Hancock, Curr. Pharm. Des. 8 (2002) 703–714.
[9] R.E.W. Hancock, R. Lehrer, Trends Biotech. 16 (1998) 82–88.
[10] A.J. deLucca, Antimicrob. Agents Chemother. 43 (1999) 1–11.
[11] R.E. Hancock, Expert Opin. Investig. Drugs 9 (2000) 1723–1729.
[12] K. Hristova, M.E. Selsted, S.H. White, J. Biol. Chem. 272 (1997) 24224–24233.
[13] W. Wang, D.K. Smith, K. Moulding, H.M. Chen, J. Biol. Chem. 273 (1998) 27438–27448.
[14] R.I. Lehrer, T. Ganz, M.E. Selsted, Cell 64 (1991) 229–230.
[15] M. Zasloff, Proc. Natl. Acad. Sci. U. S. A. 84 (1987) 5449–5453.
[16] H. Steiner, D. Hultmark, A. Engström, H. Bennich, H.G. Boman, Nature 292 (1981) 246–248.
[17] B. Bechinger, M. Zasloff, S.J. Opella, Protein Sci. 2 (1993) 2077–2084.
[18] F.M. Marassi, S.J. Opella, P. Juvvadi, R.B. Merrifield, Biophys. J. 77 (1999) 3152–3155.
[19] Z. Oren, Y. Shai, Biopolymers 47 (1998) 451–463.
[20] H.W. Huang, Biochemistry 39 (2000) 8347–8352.
[21] S.J. Ludtke, K. He, W.T. Heller, T.A. Harroun, L. Yang, H.W. Huang, Biochemistry 35 (1996) 13723–13728.
[22] K. Matsuzaki, O. Murase, N. Fujii, K. Miyajima, Biochemistry 35 (1996) 11361–11368.
[23] G.J. Boheim, J. Membr. Biol. 19 (1974) 277–303.
[24] C. Subbalakshmi, N. Sitaram, FEMS Microbiol. Lett. 160 (1998) 91–96.
[25] M. Andersson, H. Gunne, B. Agerberth, A. Boman, T. Bergman, R. Sillard, H. Jörnvall, V. Mutt, B. Olsson, H. Wigzell, A. Dagerlind, H.G. Boman, G.H. Gudmundsson, EMBO J. 14 (1995) 1615–1625.
[26] J. Andrä, M. Leippe, Med. Microbiol. Immunol. 188 (1999) 117–124.
[27] R.S. Munford, P.O. Sheppard, P.J. O'Hara, J. Lipid Res. 36 (1995) 1653–1663.
[28] E. Liepinsh, M. Andersson, J.-M. Ruysschaert, G. Otting, Nat. Struct. Biol. 4 (1997) 793–795.
[29] H. Bruhn, M. Leippe, Biol. Chem. 380 (1999) 1001–1007.
[30] D.H. Anderson, M.R. Sawaya, D. Cascio, W. Ernst, R. Modlin, A. Krensky, D. Eisenberg, J. Mol. Biol. 325 (2003) 355–365.
[31] M. Leippe, Dev. Comp. Immunol. 23 (1999) 267–279.
[32] S. Stenger, D.A. Hanson, R. Teitelbaum, P. Dewan, K.R. Niazi, C.J. Froelich, T. Ganz, S. Thoma-Uszynski, A. Melian, C. Bogdan, S.A. Porcelli, B.R. Bloom, A.M. Krensky, R.L. Modlin, Science 282 (1998) 121–125.
[33] M. Leippe, J. Andrä, H.J. Müller-Eberhard, Proc. Natl. Acad. Sci. U. S. A. 91 (1994) 2602–2606.
[34] J. Andrä, O. Berninghausen, J. Wülfken, M. Leippe, FEBS Lett. 385 (1996) 96–100.
[35] M. Leippe, Cell 83 (1995) 17–18.
[36] T. Jacobs, H. Bruhn, I. Gaworski, B. Fleischer, M. Leippe, Antimicrob. Agents Chemother. 47 (2003) 607–613.
[37] T.A. Holak, A. Engstrom, P.J. Kraulis, G. Lindeberg, H. Bennich, T.A. Jones, A.M. Gronenborn, G.M. Clore, Biochemistry 27 (1988) 7620–7629.
[38] K. Lohner, E.J. Prenner, Biochim. Biophys. Acta 1462 (1999) 141–156.
[39] D. Eisenberg, E. Schwarz, M. Komaroy, R. Wall, J. Mol. Biol. 179 (1984) 125–142.
[40] A.F.S.A. Habeeb, Methods Enzymol. 25 (1972) 457–464.
[41] R.I. Lehrer, M. Rosenman, S.S. Harwig, R. Jackson, P. Eisenhauer, J. Immunol. Methods 137 (1991) 167–173.
[42] G.R. Bartlett, J. Biol. Chem. 234 (1959) 466–468.
[43] M. Leippe, S. Ebel, O.L. Schoenberger, R.D. Horstmann, H.J. Müller-Eberhard, Proc. Natl. Acad. Sci. U. S. A. 88 (1991) 7659–7663.
[44] J. Andrä, M. Leippe, FEBS Lett. 354 (1994) 97–102.
[45] W.C. Wimley, M.E. Selsted, S.H. White, Protein Sci. 3 (1994) 1362–1373.
[46] P.R. Cullis, B. de Kruijff, Biochim. Biophys. Acta 559 (1979) 399–420.
[47] K. Matsuzaki, K. Sugishita, N. Ishibe, M. Ueha, S. Nakata, K. Miyajima, R.M. Epand, Biochemistry 37 (1998) 11856–11863.
[48] E.J. Prenner, R.N. Lewis, K.C. Neuman, S.M. Gruner, L.H. Kondejewski, R.S. Hodges, R.N. McElhaney, Biochemistry 36 (1997) 7906–7916.
[49] A.S. Ladokhin, S. Jayasinghe, S.H. White, Anal. Biochem. 285 (2000) 235–245.
[50] E.A. Burstein, N.S. Vedenkina, M.N. Ivkova, Photochem. Photobiol. 18 (1973) 263–279.
[51] J. Johansson, G.H. Gudmundsson, M.E. Rottenberg, K.D. Berndt, B. Agerberth, J. Biol. Chem. 273 (1998) 3718–3724.
[52] L. Zhang, A. Rozek, R.E. Hancock, J. Biol. Chem. 276 (2001) 35714–35722.
[53] K. Matsuzaki, K. Sugishita, N. Fujii, K. Miyajima, Biochemistry 34 (1995) 3423–3429.